Interictal hyperperfusion in the higher visual cortex in patients with episodic migraine

Lars Michels, Jeanette Villanueva, Ruth O'Gorman, Muthuraman Muthuraman, Nabin Koirala, Roman Büchler, Andreas R. Gantenbein, Peter S. Sandor, Roger Luechinger, Spyros Kollias, Franz Riederer

Angaben zur Veröffentlichung / Publication details:

Michels, Lars, Jeanette Villanueva, Ruth O'Gorman, Muthuraman Muthuraman, Nabin Koirala, Roman Büchler, Andreas R. Gantenbein, et al. 2019. "Interictal hyperperfusion in the higher visual cortex in patients with episodic migraine." *Headache: The Journal of Head and Face Pain* 59 (10): 1808–20. https://doi.org/10.1111/head.13646.

Interictal Hyperperfusion in the Higher Visual Cortex in Patients With Episodic Migraine

Lars Michels, PhD; Jeanette Villanueva, MSc; Ruth O'Gorman, PhD; Muthuraman Muthuraman, PhD; Nabin Koirala, PhD; Roman Büchler, PhD; Andreas R. Gantenbein, MD; Peter S. Sandor, MD; Roger Luechinger, PhD; Spyros Kollias, MD; Franz Riederer, MD

Background.—Migraine pathophysiology is complex and probably involves cortical and subcortical alterations. Structural and functional brain imaging studies indicate alterations in the higher order visual cortex in patients with migraine. Arterial spin labeling magnetic resonance imaging (ASL-MRI) is a non-invasive imaging method for assessing changes in cerebral blood flow (CBF) *in vivo*.

Objective.—To examine if interictal CBF differs between patients with episodic migraine (EM) with or without aura and healthy controls (HC).

Methods.—We assessed interictal CBF using 2D pseudo-continuous ASL-MRI on a 3 Tesla Philips scanner (University Hospital Zurich, Switzerland) in EM (N = 17, mean age 32.7 ± 9.9, 13 females) and HC (N = 19, mean age 31.0 ± 9.3, 11 females).

Results.—Compared to HC, EM showed exclusively hyperperfusion in the right MT+ and Cohen's *d* effect size was 0.99 (HC mean CBF ± SD: 33.1 ± 5.9 mL/100 g/minutes; EM mean CBF: 40.9 ± 9.4 mL/100 g/minutes). EM with aura (N = 13, MwA) revealed hyperperfusion compared to HC in the right MT+ and superior temporal gyrus. For MT, Cohen's *d* effect size was 1.34 (HC mean CBF ± SD: 33.1 ± 5.9 mL/100 g/minutes; MwA mean CBF: 43.3 ± 8.6 mL/100 g/minutes). For the superior temporal gyrus, Cohen's *d* effect size was 1.28 (HC mean CBF ± SD: 40.1 ± 4.9 mL/100 g/minutes; MwA mean CBF: 47.4 ± 6.4 mL/100 g/minutes). In EM, anxiety was positively associated with CBF in the parietal operculum and angular gyrus.

Conclusions.—Our results suggest that extrastriate brain regions probably involved in cortical spreading depression are associated with CBF changes in the interictal state. We conclude that ASL-MRI is a sensitive method to identify local neurofunctional abnormalities in CBF in patients with EM in the interictal state.

From the Department of Neuroradiology, University Hospital Zurich, Zurich, Switzerland (L. Michels, J. Villanueva, R. Büchler, and S. Kollias); Center for MR-Research, University Children's Hospital Zurich, Zurich, Switzerland (L. Michels and R. O'Gorman); University of Zurich, Zurich, Switzerland (A.R. Gantenbein, P.S. Sandor, and F. Riederer); RehaClinic Bad Zurzach, Bad Zurzach, Switzerland (A.R. Gantenbein and P.S. Sandor); Institute for Biomedical Engineering, ETH Zurich and University of Zurich, Zurich, Switzerland (R. Luechinger); Neurological Center Rosenhuegel and Karl Landsteiner Institute for Epilepsy Research and Cognitive Neurology, Vienna, Austria (F. Riederer); Biomedical Statistics and Multimodal Signal Processing Unit, Movement Disorders and Neurostimulation, Department of Neurology, Focus Program Translational Neuroscience (FTN), Johannes-Gutenberg-University Hospital, Mainz, Germany (M. Muthuraman and N. Koirala).

Address all correspondence to L. Michels, Department of Neuroradiology, University Hospital Zurich, Sternwartstr. 6, CH-8091 Zurich, Switzerland, email: lars.michels@usz.ch

INTRODUCTION

Migraine is a multifactorial neurovascular disorder which affects about 12% of the general population[1] and it is among the most disabling diseases.[2,3] Migraine is characterized by recurrent headache attacks, lasting 4-72 hours (untreated or unsuccessfully treated). The pain is associated with at least 2 of the 4 following features: unilateral location, pulsating quality, moderate to strong intensity, and aggravation by routine physical activity.[4] Further, it is associated with either autonomic signs (eg, nausea) or sensoriphobia (eg, photophobia). In the episodic form of migraine, headache occurs on average on less than 15 days per month, whereas in the chronic form (CM), headache occurs on ≥15/days per month for at least three consecutive months. According to the absence or presence of transient focal neurological symptoms preceding or sometimes accompanying the headache, migraine is classified as "without aura" (MwoA) or "with aura" (MwA). MwA affects about 20-30% of migraine patients.[2,5]

The lack of specificity in migraine diagnosis arises, in part, because diagnostic markers related to neurobiological mechanisms are lacking.[6] Pain sensation related to migraine is produced by multidirectional and parallel processing cascades between relay stations located in the brainstem (trigeminal nucleus caudalis) and the brain.[7,8] In analogy, the gate control theory of pain,[9,10] focused on chronic pain, postulated that neural gates in the spinal cord can be opened (or closed) by signals descending from the brain, as well as by sensory information ascending from the body. The centers in the brain linked to pain processing comprise regions associated with sensory, affective, and cognitive dimensions of pain.[11-14]

Neuroimaging studies using perfusion weighted imaging or positron emission tomography (PET) identified pathophysiological changes in the dorsolateral prefrontal-, motor-, visual cortex, and subcortical regions in patients with migraine. On the non-neuronal level, it was shown that patients with migraine (n = 153) demonstrated higher interictal flow compared to healthy controls (HC) (n = 2033) in the basilar artery using 2D phase contrast imaging.[15] Hemodynamic changes during migraine, indexed by alterations in regional cerebral blood flow (CBF), have been described using both non-invasive[5,15-17] and invasive[18-23] imaging techniques, such as PET. Sanchez del Rio and colleagues examined 13 MwoA and 6 (visual) MwA using perfusion weighted imaging during spontaneous migraine episodes.[17] Patients with MwA demonstrated hypoperfusion in the visual cortex contralateral to the hemifield defect, whereas perfusion remained constant in MwoA. In MwoA, an increased CBF related to pain was seen using PET in cortical areas and in the brainstem.[24] Brainstem activation persisted after treatment of the migraine attack with sumatriptan.[14] Afridi et al[25] reported left-lateralized brainstem (dorsal pons) activation during migraine vs the interictal state, and additional activation in the anterior cingulate cortex, posterior cingulate cortex, cerebellum, thalamus, insula, prefrontal cortex, and temporal lobes. In contrast, a deactivation (in the migraine phase) was located in the left pons, indicating that migraine involves brainstem modulations of afferent neural traffic. Using PET, activation was observed in the periaqueductal gray, dorsal pontine, and other midbrain regions in episodic MwA during the premonitory phase of a migraine.[26] In MwoA, subcutaneous application of sumatriptan did not lead to focal changes in regional CBF during or outside of an attack, as assessed by PET,[27] indicating that triptans do not necessarily lead to metabolic alterations in migraineurs.

In contrast to the described perfusion techniques, advantages of arterial spin labeling magnetic resonance imaging (ASL-MRI) include high reliability,[28,29] absolute quantification, and the avoidance of intravenous contrast administration or tracers. In an ASL-MRI case series, cerebral hyperperfusion was seen in the frontal, parietal, or visual cortex in 3 patients during the aura but in none of (eight) migraine patients interictally.[5] A single-case ASL-MRI study in a patient without aura examined changes in CBF ictally and interictally and 30 minutes after oral administration of Rizatriptan.[16] CBF during the migraine showed significant relative hypoperfusion in the bilateral thalamic and hypothalamus and hyperperfusion in the frontal cortex compared to the migraine-free state.

There has been only one previous ASL-MRI study that interictally measured CBF in adults with episodic migraine (EM).[30] Hodkinson and colleagues found a significant increase in CBF in the primary

somatosensory cortex (S1), which was positively correlated with attack frequency. Most patients showed signs of cutaneous allodynia, ie, skin hypersensitivity resulting in lower pain thresholds to stimuli, which would typically not be painful (such as hair brushing). As S1 is part of the trigemino-cortical pathway, the observed increase in perfusion in S1 may arise from adaptive or maladaptive functional plasticity. The same research group also reported hyperperfusion of S1 in adolescents with EM[31] but it was not defined if patients showed signs of aura. ASL-MRI has also been to characterize perfusion in acute confusional migraine of childhood.[32]

Hadjikhani and colleagues[33] used high-field functional MRI (fMRI) recordings during visual aura in 3 subjects.[33] The authors found an initial focal increase in the blood oxygenation level-dependent (BOLD) signal developing within extrastriate cortex (area V3A). This BOLD change progressed across the occipital cortex and then diminished, possibly reflecting cortical spreading depression (CSD). The same group also reported increased cortical thickness in MwA compared to controls in areas V5 (MT+) and V3A.[34] One of the leading hypotheses in migraine pathophysiology is that the brains of migraineurs are hyperexcitable, especially in the extrastriate cortex.[35-37] Enhanced neuronal excitation results in increased extracellular potassium. If the reuptake and other transport processes are not efficient in controlling glutamate release, a wave of CSD[38] is likely to arise because of this extracellular potassium increase. CSD is a slow, self-propagating wave of neuronal and glial depolarization, followed by long-lasting suppression of neural activity. The observed functional (Hadjikhani et al[33]) and structural (Granziera et al[34]) abnormalities might either account for or be caused by the hyperexcitability that triggers migraines. It has been suggested that CSD also plays a significant role in MwoA possibly via clinically "silent auras"[39] which is supported by the finding of cortical thickening in V3A and V5 (MT+) in MwA and MwoA.[34] It has been demonstrated that CSD is able to activate the trigemino-vascular system[40] in animal experiments, explaining the link between CSD and headache.

However, to date no study has examined if interictal changes in CBF are detectable in both episodic migraineurs with and without aura. Using ASL-MRI, we hypothesize that MwA will show hyperperfusion in extrastriate visual cortex and that hyperperfusion will be more pronounced in MwA due to a stronger manifestation of CSD associated with the aura.

MATERIAL AND METHODS

Design and Study Duration.—This is the primary analysis of the reported data using a cross-sectional design. Other imaging data (MR spectroscopy) have been collected for all participants and results will be presented elsewhere. No statistical power calculation was conducted prior to the study. The sample size was based on the available data (during the study interval) and was similar to a recent ASL study in EM patients.[30] All data were collected between December 2013 and July 2015.

Patients and Controls.—We included 17 EM and 19 HC. All EM fulfilled the ICHD-III diagnostic criteria for EM.[4] Exclusion criteria were severe psychiatric disorders, cardiac problems (eg, severe hypertension) or other neurologic disorders such as epilepsy, stroke, traumatic brain injury, neck injury, or cerebrovascular disease. All participants completed prospective headache diaries, the Migraine Disability Assessment (MIDAS)[41] and Hamilton Anxiety (HADS-A) and Depression (HADS-D) Score[42] questionnaires. The HADS questionnaire comprises 7 questions for anxiety and 7 questions for depression. For MIDAS, we assessed the attacks/month rate, ie, the attack frequency in the last 3 months prior to the MRI (eg, an attack frequency of 0.3 means 1 attack in the last 3 months). Acute and prophylactic medication was recorded prior to the study interval. Apart from migraine occurrence (days/month), we recorded aura occurrence. Patients were free from migraine attacks at least 48 hours before and after the scan. The detailed demographic data are listed in Table 1. The study was approved by the ethics committee of canton Zurich, Switzerland. All subjects provided written informed consent prior to study enrolment. HC received 40 Swiss Francs and patients received 50 Swiss Francs reimbursement for their study participation. We recruited the HC by the internal hospital webpage and by local advertisements. We specifically asked for an age-range of 20-50 years, in order to match to the expected age range of the migraineurs. In addition, we

Table 1.—Demographics and Clinical Data

	HADS-A	HADS-D	Sex	Age	Sleep	Attacks/ Month	Duration (Years)	Aura	Medication	
									Acute	Prophylactic
EM1	9	2	f	31.3	8	0.3	7	Yes	SA	
EM2	4	3	f	22.8	8	12.3	10	Yes	SA	
EM3	3	2	f	29.4	9	3.3	4	Yes (vis nausea)	T	
EM4	2	1	f	49.2	7	1.7	16	Yes	SA,T	
EM5	0	0	f	23.8	7	0.7	5	Yes	SA	
EM6	10	5	f	45.0	7	2.0	5	No	T	
EM7	9	6	m	21.8	6	9.3	12	No	T	
EM8	3	5	f	49.5	8	0.3	31	Yes (vis, mot, lang)	SA, opiate	
EM9	7	7	f	40.5	5	8.0	27	Yes	SA	
EM10	6	4	m	22.7	9	0.3	7	Yes	none	
EM11	0	0	f	26.1	8	4.7	16	No	SA	
EM12	4	2	f	35.8	7	2.0	21	No	SA	
EM13	3	2	m	32.6	7	10.0	8	Yes	none	
EM14	11	10	m	47.2	5	6.7	1	Yes	SA, T	
EM15	13	4	f	27.7	8	1.7	16	Yes (mig sans mig)	none	
EM16	4	2	f	25.9	8	3.0	7	No	SA	
EM17	2	3	f	25.2	8	1.7	11	Yes	SA, T	Riboflavin, Mg, Coenzyme Q10
Mean	**5.3**	**3.4**		**32.7**	**7.1**	**4.0**	**12.0**			
SD	**3.9**	**2.6**		**9.9**	**1.2**	**3.8**	**8.3**			
HC1	3	3	m	30.5	9					
HC2	5	1	f	20.4	1					
HC3	2	0	m	52.9	7.5					
HC4	9	1	f	55.0	6.5					
HC5	2	1	f	30.3	7.5					
HC6	6	5	m	38.2	7					
HC7	3	2	m	27.1	7.5					
HC8	1	2	f	29.4	6.5					
HC9	2	2	m	29.7	7.5					
HC10	1	0	f	24.1	6.5					
HC11	2	2	m	30.0	7					
HC12	3	1	f	28.6	7					
HC13	2	0	m	23.3	7.5					
HC14	3	0	m	39.0	6					
HC15	3	1	f	33.6	7					
HC16	6	2	f	25.3	6					
HC17	1	1	f	24.9	7					
HC18	2	1	f	25.7	8					
HC19	7	1	f	25.6	6.5					
Mean	**3**	**1**		**31**	**7**					
SD	**2.2**	**1.2**		**9.3**	**1.6**					
Between group differences										
t-test	0.067	0.004		0.644	0.528					
Chi-Square			0.238							

EM = episodic migraine; f = female; HC = healthy control; lang = language; m = male; mig = migraine; mot = motoric; SA = simple analgesic; T = triptans; vis = visual.

used age and gender as covariates in all our CBF analyses. We did not aim for a particular gender, as we had females and males with migraine. HC were screened for neurological disorders and other diseases according to exclusion/exclusion criteria based on self-reports. Regarding the HADS questionnaire, we only included

HC with a cut-off value <11, as a score of ≥11 indicates a moderate depression or anxiety,[43] respectively (see Table 1). As it is known that patients with migraine do often shown moderate to severe signs of depression or anxiety, we did not exclude any patients with HADS scores ≥ 11.

Anatomical Data.—Whole-brain 3D T1-weighted structural data were recorded on a 3 Tesla MRI Philips Ingenia scanner, equipped with a 15-element head coil. Scanning parameters were as follows 170 slices, repetition time: 8.4 ms, echo time: 3.9 ms, flip angle: 8°, voxel dimensions: 1 × 1 × 1 mm, field of view: 240 mm, scan time: 4:35 minutes. An experienced neuroradiologist (S.K.) examined all structural images for the presence of any brain abnormalities.

ASL Acquisition.—ASL data were acquired interictally using a 3 Tesla Philips 2D pseudo-continuous ASL (pCASL) sequence.[44] The acquisition parameters were: time of repetition)/time of echo = 4200/16 ms, flip angle: 90°, FOV = 240 mm, voxel size: 3 × 3 mm, 20 slices, thickness: 6 mm (no gap), imaging matrix = 80 × 80, labeling duration: 1.65 seconds, post-labeling delay: 1.53 seconds, SENSE factor: 2.5, scan duration 6:26 minutes. Background suppression was used with two pulses: 1.68 and 2.76 seconds. Equilibrium brain tissue magnetization (M0) images were recorded in a separate run for each subject using the same parameters as described for the pCASL sequence, apart from the time of repetition (10,000 ms).

ASL Analysis.—ASL images were preprocessed using the toolbox ASLtbx,[45] which was compatible with MATLAB and the SPM software package (http://www.fil.ion.ucl.ac.uk/spm/). The first step was motion correction and denoising. Subjects were excluded from subsequent analyses if any of the three translation parameters exceeded half of the voxel size (ie, 3 mm) or if rotation values exceeded 1° (see Results). Denoising included spatial smoothing with an isotropic Gaussian filter with a full-width-at-half-maximum (FWHM) of 6 mm^3 to reduce inter-individual anatomical differences and further increase the signal-to-noise ratio. The next step was pair-wise subtraction and CBF quantification using the one-compartment model.[46] All CBF images were normalized to the Montreal neurological image (MNI) template space to allow for statistical group comparison (see below).

CBF Quantification.—CBF was calculated on a voxel-wise basis according to the formula:

$$\mathrm{CBF} = \frac{60 \times 100 \times \lambda \times (M_{\mathrm{control}} - M_{\mathrm{label}})}{2\alpha T_{1\mathrm{blood}} \times M_0 (e^{\frac{-w}{T_{1\mathrm{blood}}}} - e^{\frac{-w+\tau}{T_{1\mathrm{blood}}}})}$$

$M_{\mathrm{control}} - M_{\mathrm{label}}$ reflects the subtraction of label and control images, and λ = blood brain partition coefficient for water = 0.9,[47] $T_{1\mathrm{blood}}$ = 1664 ms,[48] τ = labeling pulse train length = 1.68 seconds, α = labeling efficiency = 0.85,[44] as background suppression was used, and w (post-tagging delay) = 1.53 seconds.

The labeling efficiency and the $T1$ of blood were taken from literature values, derived from previous experimental studies.[44,48] The equilibrium magnetization of blood was calculated from the equilibrium magnetization of CSF, measured in 4 ROIs, multiplied by a correction factor for $T2^*$ decay and the relevant blood H_2O partition coefficient taken from the literature.[47] After CBF quantification, volunteers' mean CBF map (mL/100 g/minutes) was normalized to the Montreal Neurological Image (MNI) template (average of 200 realigned brain images) to allow for statistical between-group comparisons (see below). The MNI template was provided by SPM12 (Wellcome Trust, UK).

Whole-Brain CBF Analysis.—For the calculation of the CBF difference images ($M_{\mathrm{control}} - M_{\mathrm{label}}$), simple subtraction was used because it has been demonstrated to efficiently minimize spurious BOLD contaminations within the CBF signal in the case of resting-state recordings.[49] Furthermore, it has been demonstrated that simple subtraction in resting-state CBF data works with the same performance as special filtering approaches.[49]

To compare the global CBF between groups, we extracted the mean CBF for each group across 90 cortical brain regions (AAL atlas, http://neuro.imm.dtu.dk/wiki/Automated_Anatomical_Labeling) and applied unpaired two-tailed t-tests between groups (HC vs EM and HC vs MwA). In addition, we extracted the CBF for significant clusters showing a group difference to plot and compare regional CBF (unpaired two-tailed t-tests between groups). For the group analysis, we used SPM12 and set up a general linear model (GLM) in which we defined

Table 2.—Whole-Brain CBF Between-Group Comparisons

	Region	Hemisphere	MNI	*t* Value	Cluster-Size
All EM > HC	MT+ (MTG)	Right	60 -64 8	4.52	45
EM with aura > HC	MT+ (MTG)	Right	58 -64 10	6.03	159
	STG	Right	46-32 0	4.33	75

All results are reported at a statistical voxel threshold of $P < .001$ (uncorrected) with an additional cluster correction of $k > 44$ voxels to achieve $P < .050$ (cluster-corrected).
MTG = middle temporal gyrus; STG = superior temporal gyrus.

each group as one regressor of interest. First, we computed *F*-contrasts (two-sided *t*-tests), to examine if groups ("HC vs EM," "HC (using all 19 HC) vs MwA," "HC vs MwoA," and "MwA vs MwoA") differ in CBF. Next, planned contrasts were calculated (in case of significant *F*-contrasts) to examine the directionality of CBF group differences, using independent two-sample *t*-tests (one-sided with unequal variances). For all analyses, we applied a voxel-wise threshold of $P \leq .001$ ($t \geq 3.3$) with an additional cluster-correction algorithm[50] to correct for false positives (due to the multiple comparison problem). Recently, the validity of the applied method has been demonstrated, ie, fMRI inferences for spatial extent have acceptable false-positive rates.[51] Based on the ASL recording parameters, a cluster size of $k = 44$ was required to cluster correct the results at a threshold of $P \leq .05$ (cluster-corrected). Age, sex, and global CBF were included as covariates in all analyses. We subsequently ran an additional analysis without including global CBF, since global CBF could be related to regional CBF. For regions showing a significant group difference, we computed Cohen's *d* to indicate the standardized difference between two means (eg, HC – EM). Cohen's *d* was computed as

$$\text{Cohen's } d = (M2 - M1) / \text{SD}_{\text{pooled}}$$

with *M*2 and *M*1 as groups (ie, HC and EM or HC and MwA) and SD as standard deviation. Cohen's *d* effect sizes can be small (≥0.2), medium (≥0.5), or large (≥0.8).[52]

We also computed separate multiple linear regression analyses (age, sex, and global CBF were included as covariates) between voxel-specific CBF and clinical values, ie, migraine days, disease duration, anxiety, depression, and age, using a threshold of $P \leq .05$ (cluster-corrected) to minimize the likelihood of false positive results (due to multiple comparisons). These variables were used as they contain migraine related data (apart from age).

Cortical Thickness and Volume Analysis.—A cortical thickness analysis was performed for all subjects using FreeSurfer (ver.5.3.0; http://surfer.nmr.mgh.harvard.edu), the technical details of which are described in prior publications.[51,52] In brief, the automated surface-based reconstruction processing stream consists of skull stripping, Talairach space transformation, gray matter (GM), white matter (WM) and cerebral spinal fluid (CSF) boundaries optimization, segmentation of subcortical structures, tessellation, and surface deformation.[53] Cortical thickness at each vertex across the cortical mantle was calculated (in mm) as the average distance between the GM-WM surface and GM-CSF surface. The cortical volume (in mm^3) is then computed as the product of cortical thickness and vertex area. Anatomical labels based on Desikan-Killiany atlas were used for parcellating cerebral cortex for obtaining regional cortical thickness measurements. All results are reported at $P < .001$ (uncorrected).

RESULTS

Demographics and Clinical data.—EM demonstrated 4 migraine days per month (SD: 3.8; range 0.3-12.3 days) and showed moderate signs of anxiety (mean HADS-A Scores 5.3 ± 3.9) and depression (mean HADS-D-Scores 3.4 ± 2.6). Sex, age, and average duration of sleep did not differ between EM and HC (Table 1). However, EM showed significantly higher

depression scores (P = .004). Only 1 patient was on prophylactic medication during the study and 6 patients took triptans as acute medication. Twelve EM had MwA (see Table 1), although clinically it is likely that these patients also had occasional attacks without aura.

Cerebral Blood Flow.—No data were excluded as head motion parameters were in the range of acceptable translation (<3 mm) and rotation (<1°) and ASL images were artefact-free. Using a Kolmogorov-Smirnov test, we found that the global CBF was normally distributed in all HC, EM, and MwA, (P = .200, 2-tailed), warranting the use of parametric tests. As shown in Figure 1, global cortical CBF was not significantly different (all P > .050, independent samples 2-sided t-test) between HC (mean CBF ± SD: 32.6 ± 3.6 mL/100 g/minutes), MwA (mean CBF ± SD: 32.7 ± 5.1 mL/100 g/minutes), and MwoA (mean CBF ± SD: 33.3 ± 7.6 mL/100 g/minutes).

We found a main effect of group for the F-contrasts ("HC vs EM" and "HC vs MwA") in the right MT+ (F = 13.202 and F = 13.735, respectively; P < .001). As illustrated in Figure 2A, using a whole-brain analysis, EM showed exclusively hyperperfusion compared to HC in the right MT+ (unpaired 2-sample 1-sided t-test, t = −4.52, P < .001). Cohen's d effect size was 0.99 (HC mean CBF ± SD: 33.1 ± 5.9 mL/100 g/minutes; EM mean CBF: 40.9 ± 9.4 mL/100 g/minutes). As shown in Figure 2B, MwA revealed hyperperfusion in the right MT+ and superior temporal gyrus (unpaired 2-sample 1-sided t-test, t = −6.03 and t = −4.33 with P < .001, respectively). For MT+, Cohen's d effect size was 1.34 (HC mean CBF ± SD: 33.1 ± 5.9 mL/100 g/minutes; MwA mean CBF: 43.3 ± 8.6 mL/100 g/minutes). For the superior temporal gyrus, Cohen's d effect size was 1.28 (HC mean CBF ± SD: 40.1 ± 4.9 mL/100 g/minutes; MwA mean CBF: 47.4 ± 6.4 mL/100 g/minutes).

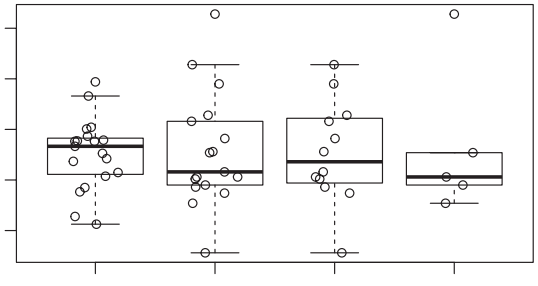

Fig. 1.—Illustration of global CBF in form of box-and-whisker plots for HC, EM, and the two EM groups: MwA and MwoA. The (bold) midline is the median of the data, with the upper and lower limits of the box being the third and first quartile (75th and 25th percentile), respectively. By default, the whiskers will extend up to 1.5 times of the interquartile range. Dots that appear outside of the whisker are outliers. Each dot represents a single subject.

A summary of the regional CBF values in the brain areas showing a group differences is provided in Figure 3 and Table 2 for all 4 groups (HC, EM, MwA, and MwoA).

In addition, the analysis without global CBF as nuisance variable (but including age and gender as covariates) demonstrated – as illustrated in Figure 4 – comparable results to the GLM including global CBF as nuisance variable, ie, EM showed hyperperfusion in the right MT+ (MTG) and MwA showed additional hyperperfusion in the right STG (using the same statistical thresholds) compared to HC.

MwoA (N = 5) did not show hyperperfusion compared to HC, even at P < .010 (uncorrected, independent samples 2-tailed t-test). No CBF differences were seen comparing MwA to MwoA (even at P < .01, uncorrected, independent samples 2-tailed t-test).

In EM, anxiety was positively associated with CBF in the left parietal operculum and right angular gyrus (parameter estimates: 2.51 + 0.56 (90% confidence interval) and 3.72 + 0.79, respectively). HADS-D and MIDAS were not significantly related to CBF.

For the contrast "EM – HC," the cortical thickness and volume analysis did not reveal significant group differences (all P ≥ .001 [uncorrected]) on the whole-brain level. For the contrast "MwA – HC," the volume of the right STG was significantly larger (P < .001, uncorrected; t-value = 3.79) in MwA compared to HC.

DISCUSSION

The present study demonstrates the utility of ASL-MRI for deriving quantitative measures of interictal CBF in patients with migraine. We found hyperperfusion in the area MT+ in migraineurs in comparison to HC, which was even more pronounced in MwA during the interictal state. We did not observe group differences in the somatosensory cortex, especially S1, as reported in a recent ASL-MRI study.[30] However, most of the patients in whom S1 perfusion changes were observed, showed allodynia and MwA were excluded.

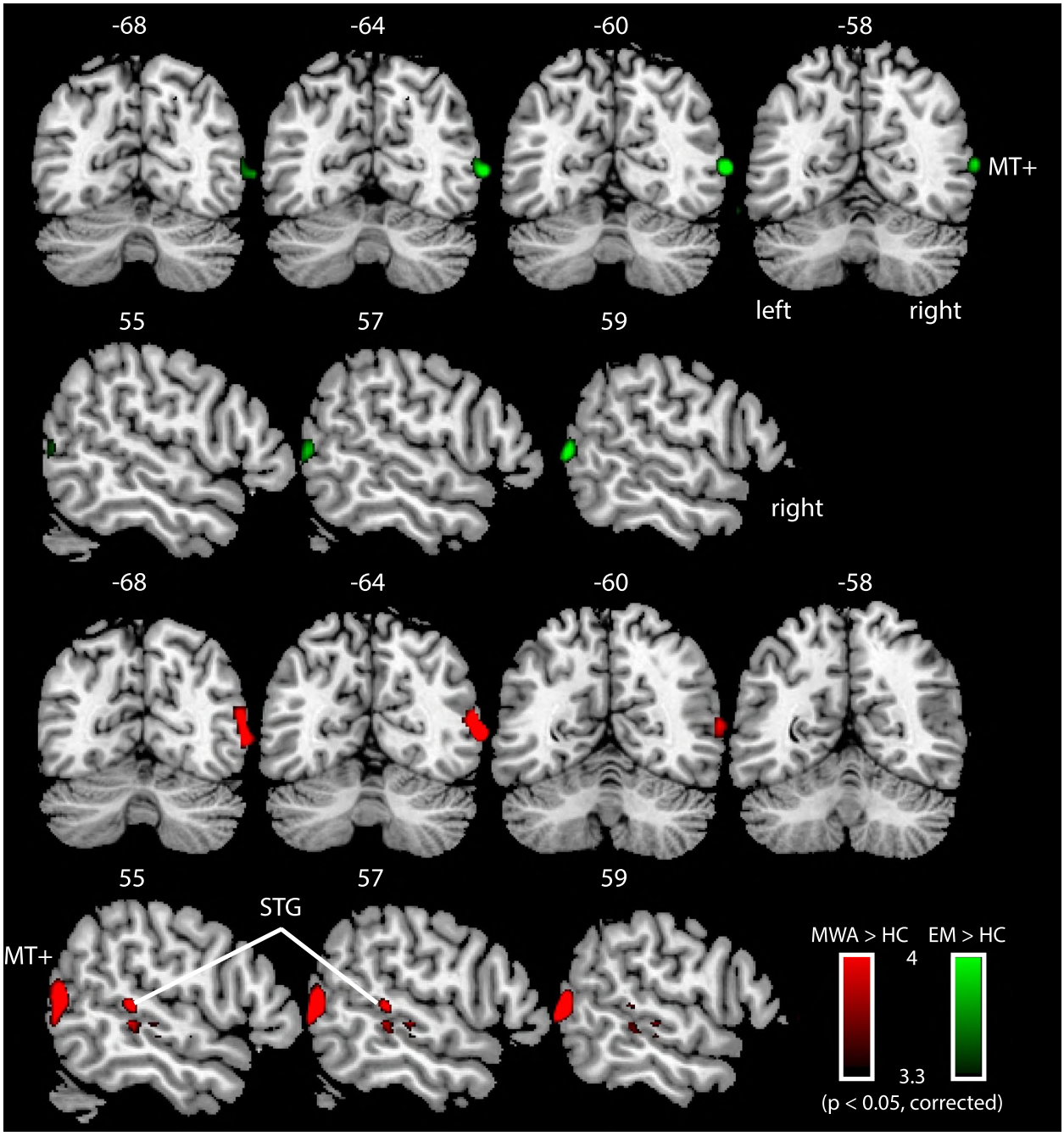

Fig. 2.—Summary of whole-brain CBF between-group differences. Hyperperfusion is seen in EM compared to HC (A). Effects are more pronounced in MwA (B). All results are reported at a statistical voxel threshold of $P < .001$ (uncorrected) with an additional cluster correction of $k > 44$ voxels to achieve a $P < .050$ (cluster-corrected). Age, gender, and global CBF were included nuisance variables in the statistical GLM.

Thus, it is unclear if CBF alterations would differ in terms of their location and spatial extent in patients with MwA and allodynia. In our study, most patients showed aura symptoms. Therefore, the observed changes in MT+ might be a feature of interictal MwA, especially since hyperperfusion was spatially more widespread for MwA compared to the whole sample of patients, including MwA and MwoA.

It might appear surprising that hyperperfusion is spatially restricted to few regions (MT+ and STG) in

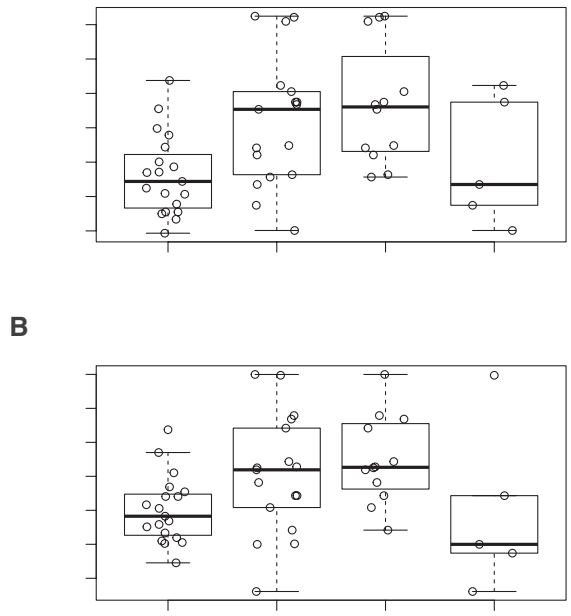

Fig. 3.—Illustration of CBF in brain regions showing group differences in form of box-and-whisker plots for each group (HC, EM, MwA, and MwoA). (A) STG, (B) MTG. The (bold) midline is the median of the data, with the upper and lower limits of the box being the third and first quartile (75th and 25th percentile), respectively. By default, the whiskers will extend up to 1.5 times of the interquartile range. Dots that appear outside of the whisker are outliers. Each dot represents a single subject.

MwA. We did not find increased cortical thickness or volume in the clusters with increased CBF, except of a larger volume in the right STG ($P < .001$, uncorrected). Thus, CBF changes may not only be related to anatomical changes. In contrast, a study with MwA found cortical thickness increases which were most pronounced in V5 and V3A.[34] In addition, a recent study revealed increased cortical thickness in V2 and V3A in females with MwA compared to controls, and increased cortical thickness of V2 in twins with MwA compared to their discordant twin pairs,[53] indicating that structural changes in visual cortex may be an inherent trait. Whether this is true for functional brain alterations needs to be addressed in future studies. The absence of cortical thickness and volume alterations in visual regions in our cohort of patients may be related to insufficient statistical power in the sample size.

Abnormal cortical excitability has been suggested to play an important role as a possible factor predisposing patients to the spontaneous CSD that has been suggested to represent the pathophysiological basis of the migraine aura.[54] The pathogenetic relevance of neuronal excitability received further support from the finding that calcium channel structure and functions are altered in familial hemiplegic migraine.[55] The notion of increased excitability of the visual cortex in the interictal phase in MwA was supported by a study using a paradigm of sound-induced flash illusions.[56] In this study, illusionary effects were decreased during the ictal and interictal phase in MwA and only during the headache phase in MWoA. In addition, using visual evoked potentials, it has been demonstrated that habituation can lead to a reduction of hyperexcitability.[57,58] It is also known that MwA but not MwoA showed significantly higher phosphene prevalence compared to controls, supporting the hypothesis of a primary visual cortex hyperexcitability in MwA.[59] Our results indicate that interictal hyperexcitability is strong in the extrastriate, especially in MT+, but not in V3A or in the early visual cortex, seen as abnormally elevated CBF in episodic MwoA and MwA.

In our study, interictal CBF increases in MT+ and temporal regions were not correlated with clinical parameters. We only find a positive association between CBF and anxiety in lateral parietal brain regions, which are part of the default mode network. In a recent study, Lo Buono and and colleagues (2017) reported increased resting-state functional connectivity in MwA compared to HC in several brain regions, including the angular gyrus[60] but no association to anxiety was reported. The angular gyrus is part of the default mode network, one of the main networks that are consistently identified when an individual is at wakeful rest and not performing an attention-demanding task. It has been reported that ictal[61] and interictal[62,63] resting-state fMRI connectivity is disturbed in the default mode network in migraine. However, the functional meaning of the observed correlation between anxiety and components of the default mode network or the parietal operculum needs to be explored in future studies.

An important question is whether the time from last migraine attack could possibly be related to the CBF, ie, whether CBF is dependent on the migraine cycle. In our study, the interval to the next attack was highly variable between participants ranging from 0.3 to 10 attacks per month. In addition, we only scanned patients

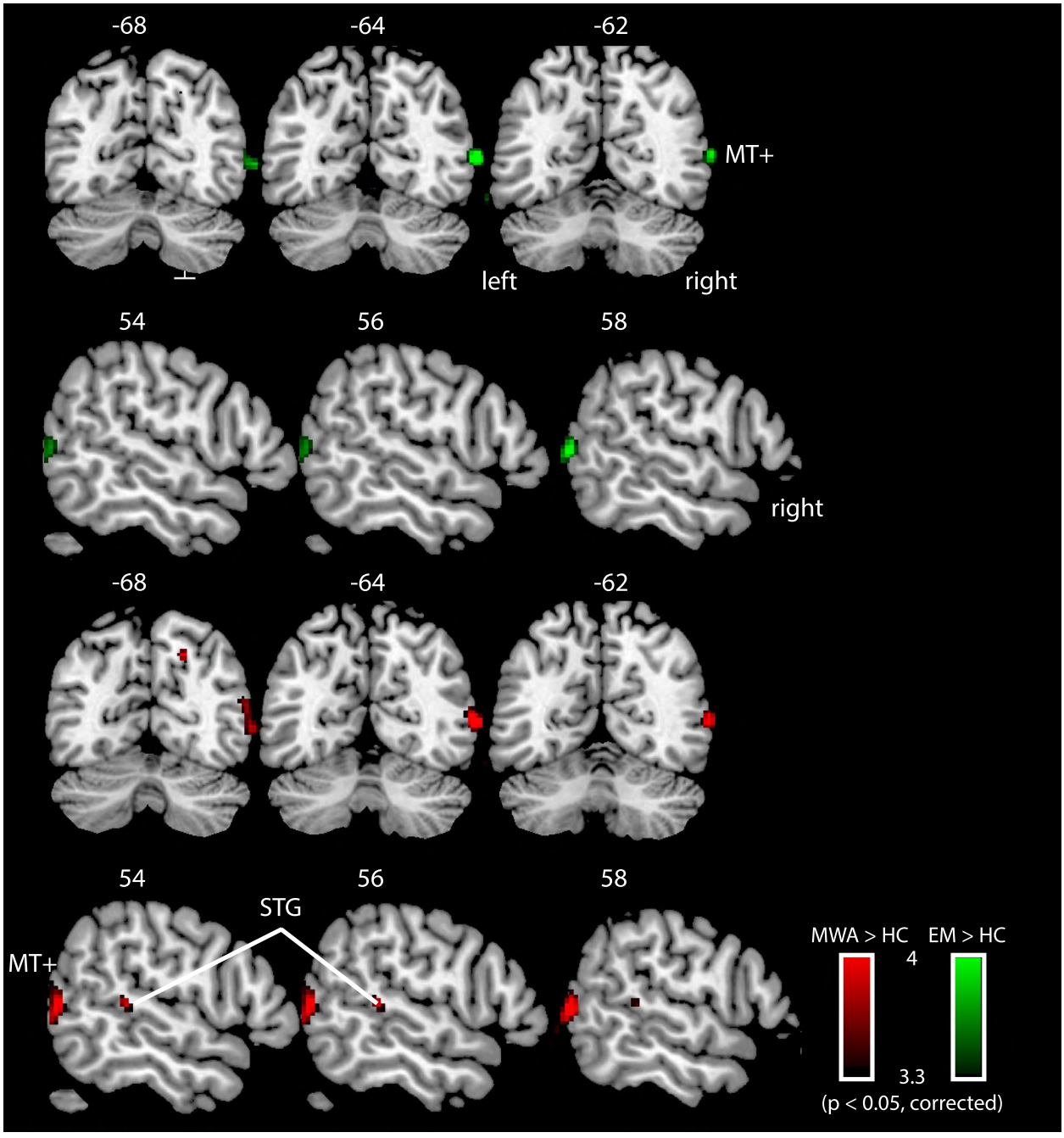

Fig. 4.—Summary of whole-brain CBF between-group differences without inclusion of global CBF as nuisance variable. Hyperperfusion is seen in EM compared to HC (A). Effects are more pronounced in MwA (B). All results are reported at a statistical voxel threshold of $P < .001$ (uncorrected) with an additional cluster correction of $k > 44$ voxels to achieve a $P < .050$ (cluster-corrected). Age and gender were included a nuisance variables in the statistical GLM.

in the interictal period, who were attack free for at least 48 hours before and after MRI measurements. Therefore, we could not perform a reasonable correlation between CBF and time to last attack. As described, we also did not observe a significant correlation between migraine days (or attack frequency) and CBF.

LIMITATIONS

The present study only investigated EM in the interictal state. Possible dynamic blood flow changes along the migraine cycle would be of great interest. In the present study, we did not systematically screen for allodynia, which may be associated with migraine.

Therefore, the results may not be comparable with a previous study in which patients frequently had allodynia.[30] Methodologically, we cannot address the question whether hyperperfusion occurred because of faster transient times or increased cerebral blood volume in EM (and MwA). The contrast "MwA – MwoA" did not show group differences, possibly due to the small sample size for both groups.

We found that between-group differences were lateralized to the right hemisphere. This could be related to the side of the preferred aura and/or headache side in the patients. Yet, we do not have information on the dominant aura and/or headache side for all patients. A possible influence of headache lateralization on interictal perfusion abnormalities should be investigated in further studies. In addition, we could not test for a relation between the presence of photophobia during attacks in patients and increased CBF compared to HC in visual/extrastriatal areas, as we did not have information on the presence of photophobia during attacks.

CONCLUSIONS

In the interictal state, hyperperfusion was found in the supposed region of CSD onset, located occipitotemporally. We conclude that ASL-MRI is a sensitive method to identify local abnormalities in CBF in episodic MwA especially, in the interictal state.

Acknowledgment: We thank Catharina Fritz-Rochner for help with patient recruitment and data analysis. We greatly appreciate the financial support by the Swiss Headache Society (Hansruedi Isler Forschungsstipendium).

STATEMENT OF AUTHORSHIP:

Category 1

(a) Conception and Design

Lars Michels, Andreas R. Gantenbein, Peter S. Sandor, Spyros Kollias, Franz Riederer

(b) Acquisition of Data

Lars Michels, Jeanette Villanueva, Franz Riederer

(c) Analysis and Interpretation of Data

Lars Michels, Ruth O'Gorman, Muthuraman Muthuraman, Nabin Koirala, Roman Büchler, Franz Riederer

Category 2

(a) Drafting the Manuscript

Lars Michels, Franz Riederer

(b) Revising It for Intellectual Content

Ruth O'Gorman, Andreas R. Gantenbein, Peter S. Sandor, Roger Luechinger, Spyros Kollias

Category 3

(a) Final Approval of the Completed Manuscript

Lars Michels, Jeanette Villanueva, Ruth O'Gorman, Muthuraman Muthuraman, Nabin Koirala, Roman Büchler, Andreas R. Gantenbein, Peter S. Sandor, Roger Luechinger, Spyros Kollias, Franz Riederer

REFERENCES

1. Manzoni GC, Stovner LJ. Epidemiology of headache. *Handb Clin Neurol*. 2010;97:3-22.
2. Lipton RB, Bigal ME, Diamond M, et al. Migraine prevalence, disease burden, and the need for preventive therapy. *Neurology*. 2007;68:343-349.
3. Vos T, Flaxman AD, Naghavi M, et al. Years lived with disability (YLDs) for 1160 sequelae of 289 diseases and injuries 1990-2010: A systematic analysis for the Global Burden of Disease Study 2010. *Lancet*. 2012;380:2163-2196.
4. Headache Classification Committee of the International Headache Society (IHS). The International Classification of Headache Disorders, 3rd edition. *Cephalalgia*. 2018;38:1-211.
5. Pollock JM, Deibler AR, Burdette JH, et al. Migraine associated cerebral hyperperfusion with arterial spin-labeled MR imaging. *Am J Neuroradiol*. 2008;29: 1494-1497.
6. Aguila ME, Lagopoulos J, Leaver AM, et al. Elevated levels of GABA+ in migraine detected using (1) H-MRS. *NMR Biomed*. 2015;28:890-897.
7. May A. Neuroimaging: Visualising the brain in pain. *Neurol Sci*. 2007;28(Suppl. 2):S101-S107.
8. Melzack R, Wall PD. Pain mechanisms: A new theory. *Science*. 1965;150:971-979.
9. Nathan PW. The gate-control theory of pain. A critical review. *Brain*. 1976;99:123-158.
10. Siegele DS. Pain and suffering. The gate control theory. *Am J Nurs*. 1974;74:498-502.
11. Cao Y, Aurora SK, Nagesh V, Patel SC, Welch KM. Functional MRI-BOLD of brainstem structures during visually triggered migraine. *Neurology*. 2002; 59:72-78.

12. Denuelle M, Fabre N, Payoux P, Chollet F, Geraud G. Hypothalamic activation in spontaneous migraine attacks. *Headache*. 2007;47:1418-1426.
13. Denuelle M, Fabre N, Payoux P, Chollet F, Geraud G. Posterior cerebral hypoperfusion in migraine without aura. *Cephalalgia*. 2008;28:856-862.
14. Weiller C, May A, Limmroth V, et al. Brain stem activation in spontaneous human migraine attacks. *Nat Med*. 1995;1:658-660.
15. Loehrer E, Vernooij MW, van der Lugt A, Hofman A, Ikram MA. Migraine and cerebral blood flow in the general population. *Cephalalgia*. 2015;35:190-198.
16. Kato Y, Araki N, Matsuda H, Ito Y, Suzuki C. Arterial spin-labeled MRI study of migraine attacks treated with rizatriptan. *J Headache Pain*. 2010;11:255-258.
17. Sanchez del Rio M, Bakker D, Wu O, et al. Perfusion weighted imaging during migraine: Spontaneous visual aura and headache. *Cephalalgia*. 1999;19:701-707.
18. Bednarczyk EM, Wack DS, Kassab MY, et al. Brain blood flow in the nitroglycerin (GTN) model of migraine: Measurement using positron emission tomography and transcranial Doppler. *Cephalalgia*. 2002;22:749-757.
19. Henry PY, Vernhiet J, Orgogozo JM, Caille JM. Cerebral blood flow in migraine and cluster headache. Compartmental analysis and reactivity to anaesthetic depression. *Res Clin Stud Headache*. 1978;6:81-88.
20. Quirico PE, Allais G, Ferrando M, et al. Effects of the acupoints PC 6 Neiguan and LR 3 Taichong on cerebral blood flow in normal subjects and in migraine patients. *Neurol Sci*. 2014;35(Suppl. 1):129-133.
21. Olesen J. Regional cerebral blood flow and oxygen metabolism during migraine with and without aura. *Cephalalgia*. 1998;18:2-4.
22. Andersson JL, Muhr C, Lilja A, Valind S, Lundberg PO, Langstrom B. Regional cerebral blood flow and oxygen metabolism during migraine with and without aura. *Cephalalgia*. 1997;17:570-579.
23. Bednarczyk EM, Remler B, Weikart C, Nelson AD, Reed RC. Global cerebral blood flow, blood volume, and oxygen metabolism in patients with migraine headache. *Neurology*. 1998;50:1736-1740.
24. Cutrer FM, O'Donnell A, Sanchez del Rio M. Functional neuroimaging: Enhanced understanding of migraine pathophysiology. *Neurology*. 2000;55:S36-S45.
25. Afridi SK, Matharu MS, Lee L, et al. A PET study exploring the laterality of brainstem activation in migraine using glyceryl trinitrate. *Brain*. 2005;128: 932-939.
26. Maniyar FH, Sprenger T, Monteith T, Schankin C, Goadsby PJ. Brain activations in the premonitory phase of nitroglycerin-triggered migraine attacks. *Brain*. 2014;137:232-241.
27. Ferrari MD, Haan J, Blokland JA, et al. Cerebral blood flow during migraine attacks without aura and effect of sumatriptan. *Arch Neurol*. 1995;52: 135-139.
28. Hodkinson DJ, Krause K, Khawaja N, et al. Quantifying the test-retest reliability of cerebral blood flow measurements in a clinical model of on-going post-surgical pain: A study using pseudo-continuous arterial spin labelling. *Neuroimage Clin*. 2013; 3:301-310.
29. Chen Y, Wang DJ, Detre JA. Test-retest reliability of arterial spin labeling with common labeling strategies. *J Magn Reson Imaging*. 2011;33:940-949.
30. Hodkinson DJ, Veggeberg R, Wilcox SL, et al. Primary somatosensory cortices contain altered patterns of regional cerebral blood flow in the interictal phase of migraine. *PLoS ONE*. 2015;10:e0137971.
31. Youssef AM, Ludwick A, Wilcox SL, et al. In child and adult migraineurs the somatosensory cortex stands out … again: An arterial spin labeling investigation. *Hum Brain Mapp*. 2017;38:4078-4087.
32. Kossorotoff M, Calmon R, Grevent D, et al. Arterial spin labeling (ASL) magnetic resonance imaging in acute confusional migraine of childhood. *J Neuroradiol*. 2013;40:142-144.
33. Hadjikhani N, Sanchez Del Rio M, Wu O, et al. Mechanisms of migraine aura revealed by functional MRI in human visual cortex. *Proc Natl Acad Sci U S A*. 2001;98:4687-4692.
34. Granziera C, DaSilva AF, Snyder J, Tuch DS, Hadjikhani N. Anatomical alterations of the visual motion processing network in migraine with and without aura. *PLoS Med*. 2006;3:e402.
35. Aurora SK, Welch KM, Al-Sayed F. The threshold for phosphenes is lower in migraine. *Cephalalgia*. 2003;23:258-263.
36. Battelli L, Black KR, Wray SH. Transcranial magnetic stimulation of visual area V5 in migraine. *Neurology*. 2002;58:1066-1069.
37. Welch KM. Contemporary concepts of migraine pathogenesis. *Neurology*. 2003;61:S2-S8.
38. Leao AAP. Spreading depression of activity in the cerebral cortex. *J Neurophysiol*. 1944;7:359-390.
39. Pietrobon D, Striessnig J. Neurobiology of migraine. *Nat Rev Neurosci*. 2003;4:386-398.

40. Lombard A, Bogdanov VB, Chauvel V, Multon S, Schoenen J. Effects of cortical spreading depression (CSD) on C-FOS expression in rat periaqueductal grey matter. *J Headache Pain*. 2010;11:S32.
41. Stewart WF, Lipton RB, Dowson AJ, Sawyer J. Development and testing of the Migraine Disability Assessment (MIDAS) Questionnaire to assess headache-related disability. *Neurology*. 2001;56:S20-S28.
42. Zigmond AS, Snaith RP. The hospital anxiety and depression scale. *Acta Psychiatr Scand*. 1983;67:361-370.
43. Stern AF. The hospital anxiety and depression scale. *Occup Med*. 2014;64:393-394.
44. Dai W, Garcia D, de Bazelaire C, Alsop DC. Continuous flow-driven inversion for arterial spin labeling using pulsed radio frequency and gradient fields. *Magn Reson Med*. 2008;60:1488-1497.
45. Wang Z, Aguirre GK, Rao H, et al. Empirical optimization of ASL data analysis using an ASL data processing toolbox: ASLtbx. *Magn Reson Imaging*. 2008;26:261-269.
46. Buxton RB, Frank LR, Wong EC, Siewert B, Warach S, Edelman RR. A general kinetic model for quantitative perfusion imaging with arterial spin labeling. *Magn Reson Med*. 1998;40:383-396.
47. Herscovitch P, Raichle ME. What is the correct value for the brain–blood partition coefficient for water? *J Cereb Blood Flow Metab*. 1985;5:65-69.
48. Lu H, Clingman C, Golay X, van Zijl PC. Determining the longitudinal relaxation time (T1) of blood at 3.0 Tesla. *Magn Reson Med*. 2004;52:679-682.
49. Liu TT, Wong EC. A signal processing model for arterial spin labeling functional MRI. *Neuroimage*. 2005;24:207-215.
50. Slotnick SD, Moo LR, Segal JB, Hart J, Jr. Distinct prefrontal cortex activity associated with item memory and source memory for visual shapes. *Cogn Brain Res*. 2003;17:75-82.
51. Slotnick SD. Cluster success: fMRI inferences for spatial extent have acceptable false-positive rates. *Cogn Neurosci*. 2017;8:150-155.
52. Cohen J. *Statistical Power Analysis for the Behavioral Sciences*. 2nd edn. New York: Lawrence Erlbaum Associate; 1988.
53. Gaist D, Hougaard A, Garde E, et al. Migraine with visual aura associated with thicker visual cortex. *Brain*. 2018;141:776-785.
54. Welch KM, Barkley GL, Tepley N, Ramadan NM. Central neurogenic mechanisms of migraine. *Neurology*. 1993;43:S21-S25.
55. Ophoff RA, Terwindt GM, Vergouwe MN, et al. Familial hemiplegic migraine and episodic ataxia type-2 are caused by mutations in the Ca^{2+} channel gene CACNL1A4. *Cell*. 1996;87:543-552.
56. Brighina F, Bolognini N, Cosentino G, et al. Visual cortex hyperexcitability in migraine in response to sound-induced flash illusions. *Neurology*. 2015;84:2057-2061.
57. Brighina F, Palermo A, Fierro B. Cortical inhibition and habituation to evoked potentials: Relevance for pathophysiology of migraine. *J Headache Pain*. 2009;10:77-84.
58. Coppola G, Di Lorenzo C, Schoenen J, Pierelli F. Habituation and sensitization in primary headaches. *J Headache Pain*. 2013;14:65.
59. Brigo F, Storti M, Tezzon F, Manganotti P, Nardone R. Primary visual cortex excitability in migraine: A systematic review with meta-analysis. *Neurol Sci*. 2013;34:819-830.
60. Lo Buono V, Bonanno L, Corallo F, et al. Functional connectivity and cognitive impairment in migraine with and without aura. *J Headache Pain*. 2017;18:72.
61. Edes AE, Kozak LR, Magyar M, et al. Spontaneous migraine attack causes alterations in default mode network connectivity: A resting-state fMRI case report. *BMC Res Notes*. 2017;10:165.
62. Coppola G, Di Renzo A, Tinelli E, et al. The resting state connectivity between default-mode network and insula encodes intensity of migraine headache. *Cephalalgia*. 2017;37:30-31.
63. Coppola G, Di Renzo A, Tinelli E, et al. Resting state connectivity between default mode network and insula encodes acute migraine headache. *Cephalalgia*. 2018;38:846-854.